ACS OMEGA

Open Access

http://pubs.acs.org/journal/acsodf

Article

Pharmacological Components and Mechanism Research on the Treatment of Myelosuppression after Chemotherapy with Danggui Jixueteng Decoction Based on Spectrum-Effect Relationships and Transcriptome Sequencing

Mingxin Guo, Jiaqi Zeng, Jing Li, Luyao Jiang, Xia Wu, Zhanyun Ren,* and Zhiqiang Hu*

Cite This: *ACS Omega* 2024, 9, 28926−28936

Read Online

ACCESS | Metrics & More | Article Recommendations | Supporting Information

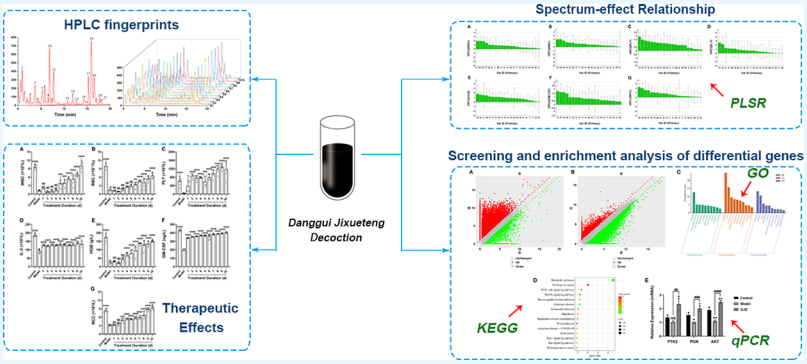

ABSTRACT: Danggui Jixueteng decoction (DJD) has been used to treat anemia for many years and has been shown to be effective. However, the mechanism of action and effective components are yet unknown. We want to search for pharmacodynamic components in DJD with therapeutic effects on myelosuppression after chemotherapy (MAC), utilizing a spectrum-effect connection study based on gray relational analysis and partial least-squares regression analysis. Transcriptome sequencing (RNA-Seq) was used to investigate the mechanism by which DJD treats MAC. In this study, fingerprints of different batches of DJD (S1−S10) were established by ultraperformance liquid chromatography-mass spectrometry (UPLC-MS), after which the resulting shared peaks were screened and identified. A total of 21 common peaks were screened through the fingerprints of different batches of DJD, and the similarity of each profile was greater than 0.92. The 21 shared peaks were identified by comparison with the standard sample and searching on a MassLynx 4.1 workstation. The rat model of MAC was established by intraperitoneal injection of cyclophosphamide, and DJD treatment was carried out in parallel with the establishment of the model. White blood cell count, red blood cell count, platelet count, interleukin-3, hemoglobin concentration, granulocyte-macrophage colony-stimulating factor, and nucleated cell count were used as efficacy indicators. Pharmacodynamic results indicated that DJD could effectively improve the pharmacodynamic indices of MAC rats. The results of gray relational analysis demonstrated eight peaks with high correlation with efficacy, which were 2, 7, 10, 14, 15, 16, 18, and 21, and the partial least-squares regression analysis showed four peaks with variable importance in projection values greater than 1, which were 10, 12, 13, and 19. RNA-Seq was used to identify DEGs in rat bone marrow cells, Gene Ontology functional enrichment and Kyoto Encyclopedia of Genes and Genomes pathway enrichment analyses of DEGs were performed. The genes related to the effects of DJD on MAC were mainly involved in the phosphatidylinositol 3-kinase/serine-threonine kinase (PI3K-Akt) signaling pathway, the mitogen-activated protein kinase signaling pathway, actin cytoskeleton regulation, focal adhesion, and Rap1 signaling pathways. The results of the RNA-Seq study were confirmed by a qPCR experiment. The effective compounds of DJD against MAC include albiflorin, paeoniflorin, gallopaeoniflorin, salvianolic acid H/I, albiflorin R1, salvianolic acid B, salvianolic acid E, benzoylpaeoniflorin, and $C_{12}H_{18}N_5O_4$. The mechanism by which DJD prevents and treats MAC might involve the control of the PI3K-Akt signaling pathway.

INTRODUCTION

Malignant tumors have become a major disease around the world that endangers human health, not only causing pain to patients but also imposing a heavy economic burden on families and society. In 2022, China and the United States are expected to have 4.82 million and 2.37 million new cancer cases and 3.21

Received: April 15, 2024
Revised: June 7, 2024
Accepted: June 10, 2024
Published: June 18, 2024

million and 640,000 new deaths, respectively.[1] As a systemic therapy, chemotherapy is an important treatment for advanced tumors with numerous and common side effects due to its low selectivity.[2] Myelosuppression after chemotherapy (MAC) is one of the most prevalent and serious side effects, causing hematopoietic dysfunction, mainly in the form of significant decreases in white blood cell (WBC) count, platelet (PLT) count, red blood cell (RBC) count, and nucleated cell count (NCC), which may lead to bleeding and infections.[3] Currently, transfusions of red blood cells or platelets or the subcutaneous injection of stimulating factors are the mainstays of treatment. However, the above treatments can cause a range of side effects and greatly increase the financial burden on patients, leading many patients to seek other treatments to supplement or replace them.

In recent years, traditional Chinese medicine (TCM) has been widely used in the clinical treatment of MAC because of its synergistic effects, reduced toxicity, and immunomodulatory effects, and TCM has achieved certain clinical efficacy.[4,5] Danggui Jixueteng decoction (DJD), the original formula from the book "Traditional Chinese Medicine Traumatology", consists of six Chinese herbs, namely, *Angelica sinensis* radix, *Spatholobi caulis*, *Rehmanniae radix* praeparata, *Longan arillus*, *Paeoniae radix* alba, and *Salviae Miltiorrhizae* Radix et Rhizoma, which are widely used to treat periarthritis, cervical spondylosis, and heel pain due to their ability to replenish qi and tonify blood, activate blood circulation and remove blood stasis, and activate collaterals to relieve pain.[6] The improvement of *Salviae Radix* on side effects induced by chemotherapy has been validated by Cho et al.,[7] while Peng et al. revealed the therapeutic effect of *Spatholobi caulis* on bone marrow suppression.[8] In addition, the tonifying qi and blood nourishing effects of *Angelica sinensis* have been repeatedly studied.[9,10] In this preliminary study, we constructed a rat model to verify the therapeutic effect of DJD on MAC and explored the core targets, key compounds, major biological processes, and signaling pathway related to treatment using network pharmacology, molecular docking, and metabolomics.[11] However, as a TCM compound preparation, the chemical composition of DJD is complex and diverse, and the database-based prediction results do not fully represent the actual situation. Furthermore, the specific molecular mechanism of DJD in treating MAC is unknown.

Spectrum-effect relationship analysis is a common method that combines chemical characterization, pharmacodynamics, and statistical analysis to discover the core active ingredients.[12] Spectrum-effect relationship analysis based on fingerprint data and bioactivity studies is a scientific approach for explaining the material basis of the pharmacological effects of TCM and developing quality control procedures for TCM.[13] In recent years, an increasing number of studies have shown that spectrum-effect relationship analysis plays a crucial role in the screening of pharmacodynamic substances,[14] ingredient compatibility,[15] processed products,[16] and specific toxic ingredients in Chinese medicine.[17] However, the chemical components of DJD are unknown, and there is no convincing quality control method for DJD. Therefore, to further identify the main active ingredients related to the therapeutic effects of DJD, the fingerprints were established by UPLC-MS, and the main active ingredients were preliminary identified by gray relational analysis (GRA) and partial least-squares regression (PLSR). Additionally, transcriptome sequencing (RNA-Seq) was employed to investigate the mechanism of action of DJD, providing a research basis for its clinical application.

MATERIALS AND METHODS

Reagents and Instruments. Different batches of *Angelica sinensis* radix, *Spatholobi caulis*, *Rehmanniae radix* praeparata, *Longan arillus*, *Paeoniae radix* alba, and *Salviae Miltiorrhizae* Radix et Rhizoma (Kangmei Pharmaceutical Co., Ltd.) were identified by pharmacists according to the standards of the Chinese Pharmacopoeia. Paeoniflorin (Lot: M28GB143089), procyanidin (Lot: N12HB201033), procyanidin B2 (Lot: F18HB175826), salvianolic acid B (Lot: A18IB223269), catechin (Lot: S01HB191501), lithospermic acid (Lot: D09GB165792), and cyclophosphamide (Lot: F13IS206786) were obtained from Shanghai Yuanye Biological Products Co., Ltd. Interleukin-3 (IL-3) and granulocyte-macrophage colony-stimulating factor (GM-CSF) ELISA kits were obtained from Jiangsu Meimian Industrial Co., Ltd. RNA rapid extraction solution (Wuhan Servicebio Technology Co., Ltd.) was used. The acetonitrile, methanol, and formic acid used for mass spectrometry were pure (CNW, Germany); the other reagents used were analytically pure; and the water used was ultrapure water.

Ultraperformance liquid chromatography coupled with Q-TOF mass spectrometry (UPLC/Q-TOF-MS) was used with a MassLynx 4.1 data software processing system (Waters, USA). An XN9500 fully automated hematology analyzer (Sysmex, Japan) was used. SIMCA-P 14.0 (Sweden, Umetrics) and CFX Connect Fluorescent Quantitative PCR instrument (Bio-Rad, USA) were used.

Establishment of DJD Fingerprints. *Sample Preparation.* According to the book "Traditional Chinese Medicine Traumatology," a group of herbs constituting DJD was soaked in 2 L of purified water for 1 h, heated to boiling, decocted for 30 min, and filtered. The filter residue was boiled in six times the amount of distilled water for 30 min and filtered. The two filtrates were combined, added to a rotary evaporator, and concentrated under reduced pressure to obtain the test solution. The constituents of DJD and the Latin, English, and Chinese Pinyin herbs are presented in Table 1.

Table 1. Constituents of DJD and the Latin, English, and Chinese Pinyin Herbs

number	Latin	English	Chinese pinyin	content
1	*Angelica sinensis* (Oliv.) Diels	*Angelicae sinensis* radix	Danggui (DG)	15 g
2	*Spatholobus suberectus* Dunn	*Spatholobi caulis*	Jixueteng (JXT)	15 g
3	*Rehmannia glutinosa* Libosch. Libosch.	*Rehmanniae Radix* Praeparata	Shudihuang (SDH)	15 g
4	*Paeonia lactiflora* Pall.	*Salviae Miltiorrhizae* Radix et Rhizoma	Baishao (BS)	9 g
5	*Salvia miltiorrhiza* Bge.	*Salviae Miltiorrhizae* Radix et Rhizoma	Danshen (DS)	9 g
6	*Dimocarpus longan* Lour.	*Longan arillus*	Longyanrou (LYR)	6 g

Liquid Phase and Mass Spectrometry Conditions. Column: Waters CORTECS UPLC-C18 (2.1 mm × 100 mm, 1.6 μm); mobile phase: composition A: 0.1% formic acid solution; B: acetonitrile; gradient elution procedure: 0−2.0 min at 5% B; 2.0−5.0 min at 5−15% B; 5.0−8.0 min at 15% B; 8.0−12.0 min at 15−30% B; 12.0−15.0 min at 30% B; 15.0−17.0 min at 30−75% B; 17.0−19.0 min at 75−95% B; 19.0−20.0 min at 95% B. Flow rate: 0.3 mL/min; column temperature: 30 °C; and injection volume: 3 μL.

https://doi.org/10.1021/acsomega.4c03641
ACS Omega 2024, 9, 28926−28936

Ion source: ESI, positive ion mode acquisition; real-time mass number correction with leucine-enkephalin (10 μg/mL); Sample cone: 15 V; capillary: 2 800 V; desolvation temperature: 300 °C; source temperature: 100 °C; crushing energy: 15 V; scanning range: 100−2000 Da.

Establishment of Fingerprints. Ten batches of DJDs (S1−S10) were obtained by combining them using the random number table method. The DJD sample solutions were prepared according to Section 2.2.1; the samples were injected for determination according to Section 2.2.2; and the chromatographic data of each batch of samples were recorded. For investigation, the data of 10 DJD batches were imported into the similarity evaluation system of chromatographic fingerprints of traditional Chinese medicine (2012 edition).

Composition Identification Strategy. By searching the related literature on six Chinese herbs in the DJD, we combined the chemical books and ChemSpider databases to establish a chemical composition information database. According to the established analysis methods, DJD, *Angelica sinensis* radix, *Spatholobi caulis*, *Rehmanniae radix* praeparata, *longan arillus*, *Paeoniae radix* alba, and *Salviae Miltiorrhizae* Radix et Rhizoma were detected. According to the retention time, fragmentation rule of mass spectrometry, and comparison with standard samples, the target compounds corresponding to each chromatographic peak were determined.

Pharmacodynamic Evaluation. *Animal Model.* The animal protocol conformed to the guidelines for the care and use of laboratory animals published by the US National Academy of Sciences and the US National Institutes of Health and the principles of laboratory animal care established by the National Institute for Medical Research. The study was conducted in accordance with the ARRIVE guidelines. All animal assays were approved by the Institutional Animal Care and Use Committee (approval number: HTDW-202306003). Male SD rats (7 weeks of age, weighing approximately 180−220 g) were obtained from Vitonglihua Experimental Animal Technology Co., Ltd. (Beijing, China).

Typical laboratory conditions of 12 h of darkness and 12 h of light were used, and food and water were freely available to the rats. SD rats were randomly divided into 12 groups after adaptive feeding for 1 week. The control group, model group, and 10 DJD groups were included (n = 6). Except for those in the control group, rats in the model group and DJD group were intraperitoneally injected with cyclophosphamide solution at 30 mg/kg/day for 5 days, while rats in the control group were intraperitoneally injected with normal saline in the same way. The control group and model group were given saline at a dose of 6.21 g/kg. On the fifth day, 30 min after each administration, one group of DJD rats was sacrificed by deep anesthesia, and the samples to be tested were collected until the 15th day.

Sample Collection. An intraperitoneal dose of 3% pentobarbital sodium (30 mg/kg) was used to anesthetize the rats. Following successful anesthesia, 3−5 mL of blood was drawn from the venous plexus of the inner canthus and placed in a test tube. An automated biochemical analyzer was used to immediately assess blood samples in anticoagulant tubes. The blood samples in the test tube were kept at 4 °C for 2 h before being centrifuged at 4500 r/min for 10 min, after which the supernatant was collected. Following blood collection, the rats were sacrificed under deep anesthesia, and the femurs on both sides were removed under aseptic conditions, as were the muscles. Serum and plasma were packaged separately and stored at −80 °C to avoid repeated freezing and thawing.

Pharmacodynamic Index Determination. The numbers of RBC, WBC, HGB, and PLT in rat peripheral blood were quantified using an automated biochemical analyzer. The levels of IL-3 and GM-CSF in rat serum were measured using the kit's instructions. Both ends of the left femur were removed with scissors, bone marrow cells were flushed with phosphate buffer into the centrifuge tube, and the bone marrow cavity was washed repeatedly until it was translucent. The flushing fluid was centrifuged at 4 °C at 12,000 r/min for 10 min before being added to 0.5 mL of RPMI-1640 media to resuspend the cells. The nucleated cells in the bone marrow were observed and counted under a microscope after 20 μL of cell suspension was placed on the cell counting plate.

Spectral-Effect Relationship Analysis. The spectral-effect relationship was investigated using gray relational grade analysis (GRA) and partial least-squares regression (PLSR). The correlation coefficients between seven pharmacodynamic indices (WBC, RBC, HGB, PLT, IL-3, GM-CSF, and NCC) and 21 common peaks were investigated in this work to establish the primary active components associated with pharmacological effects.

In this experiment, the common peak area of different batches of DJD was used as the independent variable X, which was recorded as $X1$, $X2$, $X3$, $X4$,...Xn, and the mean values of the pharmacodynamic factors measured at different times were used as the dependent variable Y, denoted as $Y1$, $Y2$, $Y3$, $Y4$,...Yn. The absolute difference series, correlation coefficients, and correlation (r) were calculated by the SPSSPro (https://www.spsspro.com/) online data processing system by dimensionless processing of the raw data. The greater the connection between the components and effectiveness, the greater the absolute value of the correlation coefficient. The calculation steps are as follows:

(1) Dimensionless processing: the reference sequence and the comparison sequence are dimensionless by means of the mean method.

(2) Find the gray correlation coefficient: for the reference sequence, there are several comparative sequences, and the gray correlation coefficient $[\xi_i(k)]$ between each comparative sequence and the reference sequence can be calculated by the following formula:

$$\xi_i(k) = \frac{\min \Delta i(k) + \rho_{\max}\Delta i(k)}{\Delta i(k) + \rho_{\max}\Delta i(k)}$$

ρ is the resolution coefficient, generally between 0 and 1, usually 0.5; $\Delta i(k)$ represents the absolute difference between the comparison sequence and the reference sequence; $\min\Delta i(k)$ and $\max\Delta i(k)$ represent the minimum and maximum of the absolute value of the difference in the comparison sequence, respectively.

(3) Calculation of correlation degree:

$$r_i = \frac{1}{n}\sum_{k=1}^{n}\xi_i(k),\ \ k = 1, 2, 3, \ldots n$$

The raw data were imported into SIMCA-P 14.0 for PLSR analysis. A coefficient analysis was performed after numerous repetitions of the main components were extracted, and the matching regression coefficient was calculated. When the coefficient was positive, the component's response value was favorably associated with its efficacy. Otherwise, the component's response value was negatively connected to its efficacy.

https://doi.org/10.1021/acsomega.4c03641
ACS Omega 2024, 9, 28926−28936

Variable importance in projection (VIP) analysis was used to further identify key components. The components with VIP values greater than 1 suggested that the independent variable had a better ability to explain the dependent variables, indicating that the effective components were significant.

Transcriptomic Sequencing. *General Operating Process.* Three samples were selected at random from the normal, model, and DJD groups for RNA-Seq. Total RNA was isolated from bone marrow cells using a TRIzol kit, and rRNA was removed using the probe technique after the quality was verified. The cDNA library was then amplified and sequenced on the Illumina platform using RNA fragment sequencing, strand-specific synthesis of cDNA, connecting splicing sequencing, digestion of two-strand cDNA, and PCR enrichment.

Screening and Enrichment Analysis of Differentially Expressed Genes. DESeq2 software was used to test for lncRNA differences across groups with $|\log2FC| \geq 1$ and $P < 0.05$. To gain a thorough understanding of the biological processes, molecular functions, and cell components associated with the DEGs, we used the Gene Ontology (GO) database (http://geneontology.org/) for gene enrichment analysis and the Kyoto Encyclopedia of Genes and Genomes (KEGG) database for metabolic pathway enrichment analysis.

qPCR Test. After sequencing, the differentially expressed genes in the remaining bone marrow cell samples were confirmed via qPCR. The following methods were used to extract RNA: cDNA was generated through reverse transcription, target and internal reference gene expression levels were detected via qPCR, and relative gene expression was calculated via the $2^{-\Delta\Delta CT}$ method. Table 2 contains primer sequences.

Table 2. Primer Sequences

name		
β-actin	F: TGCTATGTTGCCCTAGACTTCG	240
	R: GTTGGCATAGAGGTCTTTACGG	
PTK2	F: GCTTTGAAGTTGGGTTGTTTGG	189
	R: CTGCCTGAATGTTTGCTGGATC	
AKT	F: CGACGTAGCCATTGTGAAGGAG	173
	R: ATTGTGCCACTGAGAAGTTGTTG	
PI3K	F: GTAAGGGCCATTGCAGTTCAG	201
	R: GGACTGGGCTATCTCACTTCGC	

Statistical Methods. SPSS 17.1 software was used for data processing, and the data were expressed as the average ± standard deviation. A one-way analysis of variance was used to compare two groups, and $P < 0.05$ indicated a significant difference.

RESULTS

UPLC-MS Fingerprints of DJD. The fingerprints of 10 batches of DJD were established by UPLC-MS. As shown in the total ion chromatogram (Figure 1A) and the overlay fingerprints of S1−S10 (Figure 1B), there were 21 common peaks in different batches of DJD. The similarity of each profile was greater than 0.92 (Table 3). The RSDs of the total peaks and peak areas were calculated to be <0.17 and <2.98%, respectively, which indicated good precision and reproducibility of the method.

Ingredient Identification. In accordance with Section 2.2.1, *Angelicae sinensis* radix, *Spatholobi caulis*, *Rehmanniae Radix* Praeparata, *Salviae Miltiorrhizae* Radix et Rhizoma, *Paeoniae Radix* Alba, and *Longan arillus* were extracted separately, and unknown compounds were identified. The herbal origin of the major peaks in the DJD fingerprints could be determined based on the retention times. Relevant information obtained from the literature review and application of an online database search was summarized, including molecular formula, substance structure, relative molecular mass, and cleavage pattern, and then individual peaks were searched using the MassLynx 4.1 workstation to obtain molecular formulas with an error range of $\leq 5.0 \times 10^{-6}$. For substances with the same molecular weight and similar secondary fragments, control samples were used for identification. Eventually, 21 shared peaks in the DJD fingerprint profile were identified, and the results are presented in Table 4.

Therapeutic Effects of DJD on MAC. In a previous study of the effects of different doses of DJD on pharmacodynamics, we found that when the dose of DJD was 6.21 g/kg, the related indices of MAC rats were significantly improved. As shown in Figure 2, compared with those in the normal group, the WBC, RBC, HGB, PLT, IL-3, GM-CSF, and NCCin the bone marrow in the model group decreased significantly. After treatment with DJD, the blood indices in all groups were significantly greater than those in the model group. With prolonged intervention, the hematopoietic function of the MAC model rats in the DJD group improved significantly ($P < 0.01$, compared with that of the model group). The results are shown in Table S1 and indicated that DJD could effectively improve the peripheral hemogram indices of MAC rats, and the above seven pharmacodynamic indices were selected as indicators for spectrum-effect correlation analysis.

Spectrum-Effect Relationship. *Gray Relational Analysis.* The gray system theory examines the degree of correlation between the factors of the system through the quantitative analysis of the dynamic development process of the system, and its main method is to construct the degree of correlation based on the similarity of the development process or magnitude between two sequences and to construct the degree of correlation by reflecting the similarity of the development trend of two sequences. This method of detecting the degree of influence between two factors through the similarity of trends or curve shapes can inform decision-making and the judgment of the main factors.[18]

As shown in Tables S2−S8, there were 20, 17, 18, 21, 8, 20, and 19 peaks with a correlation greater than 0.6 with WBC, RBC, PLT, IL-3, HGB, GM-CSF, and NCC, respectively. Considering the seven pharmacological indicators mentioned above, there were a total of eight peaks highly correlated with them: numbers 2, 7, 10, 14, 15, 16, 18, and 21.

Partial Least-Squares Regression Analysis. Variable importance in projection (VIP) analyses were used to identify additional key elements. The independent variables of components with higher VIP values better explained the dependent variable. As shown in Figure 3, the peak correlations with WBC and VIP values greater than 1 were 12, 13, 19, 17, 9, and 20; the correlations with RBC and VIP values greater than 1 were 12, 19, 13, 17, and 10; the correlations with PLT and VIP values greater than 1 were 12, 13, 17, 9, 6, 19, 5, 18, and 10; the correlations with IL-3 and VIP values greater than 1 were 12, 13, 2, 8, 19, and 10; the correlations with HGB and VIP values greater than 1 were 12, 13, 2, 19, 17, 3, 9, and 16; the correlations with GM-CSF and VIP values greater than 1 were 12, 17, 13, 19, and 2; and the correlations with NCC and VIP values greater than 1 were 12, 13, 19, 17, 10, 9, and 20. Overall, peaks 10, 12,

https://doi.org/10.1021/acsomega.4c03641
ACS Omega 2024, 9, 28926−28936

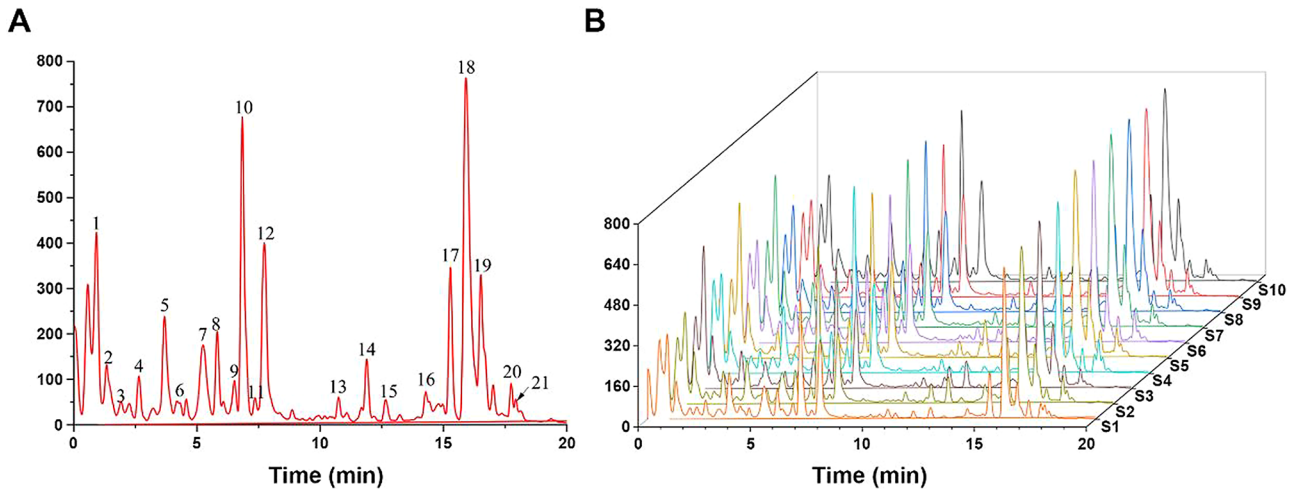

Figure 1. UPLC-MS fingerprints of DJD. (A) Total ion chromatogram of UPLC-MS in positive ion mode. (B) Overlay of UPLC-MS fingerprints of 10 batches of DJDs (S1−S10).

Table 3. Similarity of DJD Fingerprint Profiles across Batches

	S1	S2	S3	S4	S5	S6	S7	S8	S9	S10	control
S1	1.0000	0.9860	0.9850	0.9880	0.9670	0.9790	0.9760	0.9720	0.9910	0.9860	0.9950
S2	0.9860	1.0000	0.9790	0.9850	0.9330	0.9870	0.9480	0.9810	0.9870	0.9720	0.9880
S3	0.9850	0.9790	1.0000	0.9860	0.9730	0.9710	0.9620	0.9700	0.9830	0.9800	0.9910
S4	0.9880	0.9850	0.9860	1.0000	0.9670	0.9870	0.9780	0.9880	0.9960	0.9910	0.9980
S5	0.9670	0.9330	0.9730	0.9670	1.0000	0.9280	0.9790	0.9300	0.9620	0.9790	0.9720
S6	0.9790	0.9870	0.9710	0.9870	0.9280	1.0000	0.9500	0.9970	0.9830	0.9700	0.9870
S7	0.9760	0.9480	0.9620	0.9780	0.9790	0.9500	1.0000	0.9460	0.9800	0.9920	0.9810
S8	0.9720	0.9810	0.9700	0.9880	0.9300	0.9970	0.9460	1.0000	0.9810	0.9680	0.9850
S9	0.9910	0.9870	0.9830	0.9960	0.9620	0.9830	0.9800	0.9810	1.0000	0.9910	0.9970
S10	0.9860	0.9720	0.9800	0.9910	0.9790	0.9700	0.9920	0.9680	0.9910	1.0000	0.9930
control	0.9950	0.9880	0.9910	0.9980	0.9720	0.9870	0.9810	0.9850	0.9970	0.9930	1.0000

Table 4. Identification of Peaks by UPLC-MS

number	retention time	identification	molecular	experimental mass *m/z*	theoretical mass *m/z*	error/ppm	MS/MS
1	0.88	adenosine	$C_{10}H_{13}N_5O_4$	268.1048	268.1046	0.07	136
2	1.32	unknown	$C_{12}H_{18}N_5O_4$	328.1255	328.1257	−0.06	264, 292, 310
3	1.88	unknown	$C_{12}H_{18}N_5O_5$	595.1533	595.1537	−0.07	247, 427
4	2.61	unknown	$C_{15}H_{22}O_8$	331.1382	331.1393	−0.33	205, 331
5	3.68	procyanidin B1/B3	$C_{27}H_{30}O_{14}$	579.1322	579.1350	−0.48	427, 409, 291, 247
6	4.34	(+)-catechin[a]	$C_{15}H_{14}O_6$	291.0869	291.0892	−0.79	165, 139
7	5.17	procyanidin B1/B3	$C_{30}H_{26}O_{12}$	579.1540	579.1503	0.64	427, 409, 291, 247
8	5.8	procyanidin B2[a]	$C_{30}H_{26}O_{12}$	579.1560	579.1503	0.98	427, 409, 291, 247
9	6.5	procyanidin C1/C2	$C_{45}H_{38}O18$	867.2163	867.2136	0.31	598, 291
10	6.82	albiflorin	$C_{23}H_{28}O_{11}$	481.1729	481.1710	0.39	319, 301, 197, 105
11	7.32	glycyroside	$C_{27}H_{30}O_{13}$	563.1717	563.1765	−0.85	393, 291
12	7.7	paeoniflorin[a]	$C_{23}H_{28}O_{11}$	498.1704	498.1737	−0.66	301, 197, 179
13	10.6	galloylpaeoniflorin	$C_{30}H_{32}O_{15}$	633.1813	633.1819	−0.09	319, 179
14	11.89	salvianolic acid H/I	$C_{27}H_{22}O_{12}$	539.1135	539.1190	−1.02	521, 323, 269, 181
15	12.6	jionoside B1	$C_{37}H_{50}O_{20}$	815.3051	815.2974	0.94	339
16	14.3	albiflorin R1	$C_{23}H_{28}O_{11}$	481.1751	481.1710	0.85	319, 301, 197, 179
17	15.26	lithospermic acid[a]	$C_{27}H_{22}O_{12}$	539.1260	539.1190	1.30	431, 341
18	15.9	salvianolic acid B[a]	$C_{36}H_{30}O_{16}$	719.1599	719.1622	−0.32	521, 493, 323, 181
19	16.5	salvianolic acid E	$C_{36}H_{30}O_{16}$	719.1647	719.1622	0.35	521, 323, 181
20	17.73	benzoyloxypaeoniflorin	$C_{30}H_{32}O_{11}$	602.1904	602.1955	−0.85	585, 319, 301, 267
21	17.92	benzoylpaeoniflorin	$C_{30}H_{32}O_{12}$	585.2007	585.2031	−0.41	319, 301, 267, 151

[a]Compare with standard substance.

13, and 19 were the main components of the MAC treated with DJD.

In summary, the joint action of multiple components contributed to the therapeutic effect of DJD on MAC. The

https://doi.org/10.1021/acsomega.4c03641
ACS Omega 2024, 9, 28926−28936

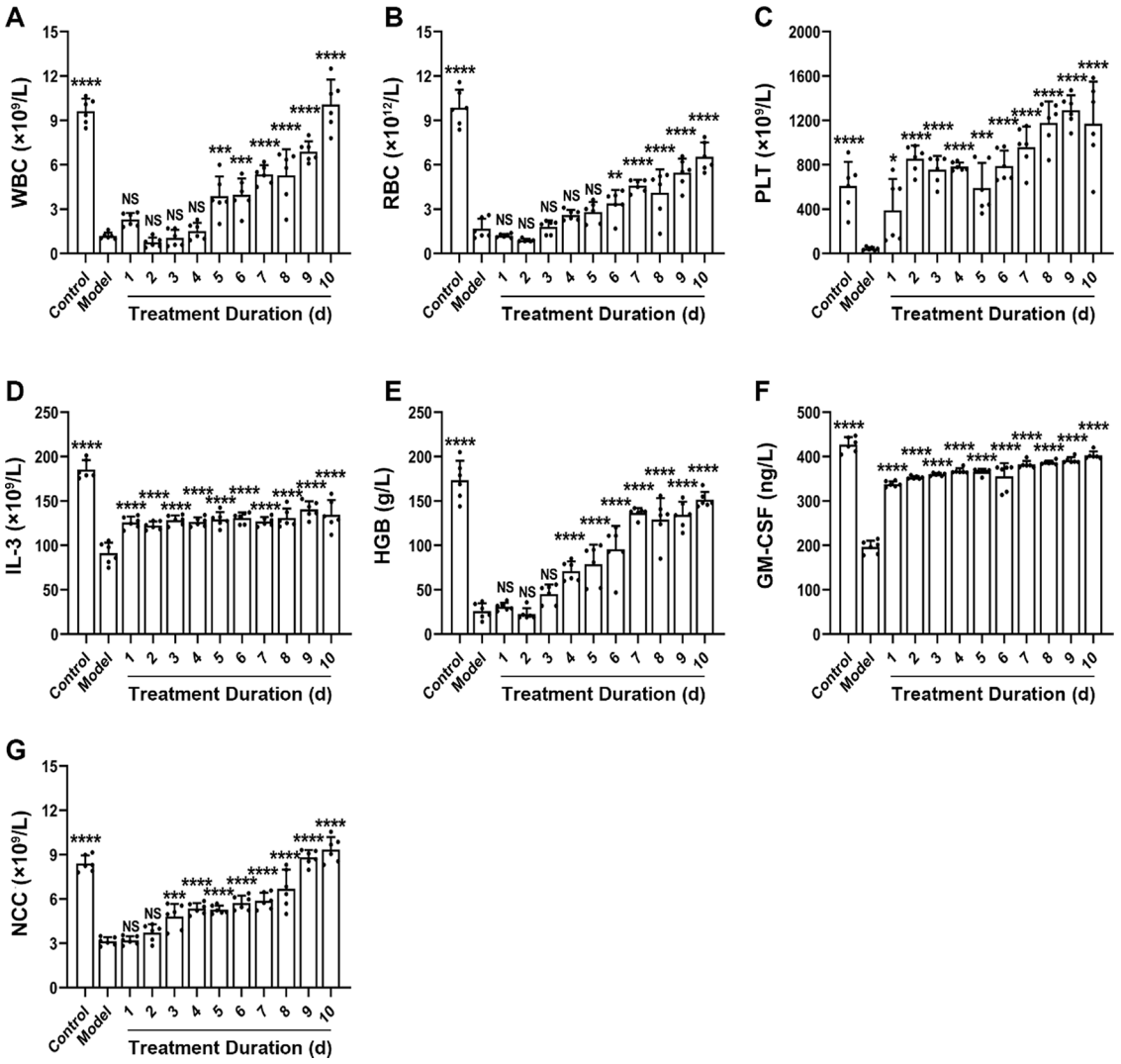

Figure 2. Therapeutic effects of DJD on MAC. (A) WBC, (B) RBC, (C) PLT, (D) IL-3, (E) HGB, (F) GM-CSF, and (G) NCC in rats with MAC (mean ± SD, $n = 6$). Compared with the model group, NS group: $p > 0.05$, $^{*}p < 0.05$, $^{**}p < 0.01$, $^{***}p < 0.001$, $^{****}p < 0.0001$; ANOVA.

main active components of DJD that exerted therapeutic effects on MAC were screened using a gray correlation >0.7 and a VIP value >1. The results indicated that albiflorin (10), paeoniflorin (12), galloylpaeoniflorin (13), salvianolic acid H/I (14), albiflorin R1 (16), salvianolic acid E (19), benzoylpaeoniflorin (21), and $C_{12}H_{18}N_5O_4$ (2) were the major pharmacodynamic components.

Screening and Enrichment Analysis of Differentially Expressed Genes. *Quality Assessment of Samples.* In the established sequencing library, the proportion of base masses above Q20 in nine sets of samples was greater than 99.00%, and the proportion exceeding Q30 was greater than 96.65%, indicating that the samples were stable and that the sequencing findings were reliable.

Screening Differentially Expressed lncRNAs. As shown in Figure 4, RNA-Seq revealed 7388 differentially expressed lncRNAs in the model group compared to the normal group and 3629 differentially expressed lncRNAs in the DJD group compared to the model group. The distance threshold between the lncRNAs and known protein-coding genes was set to within 100 kb upstream and downstream of the lncRNAs, after which the target genes controlled by the lncRNAs were identified. The Venn diagram revealed 5744 differential target genes in the different groups.

Enrichment Analysis of Common Differentially Expressed Genes. GO function and KEGG pathway enrichment analyses were performed on the DEGs involved in the DJD treatment of MAC. A screening standard of $P < 0.05$ was used, and gene ratios were used for sorting. As shown in Figure 5A, the functional enrichment of biological process (BP) terms largely included transport, differentiation, cell cycle, and cell adhesion; cell component (CC) terms included the cytoplasm, nucleus, and cytoskeleton, among others. The molecular function (MF) category mainly included transferase, kinase, RNA-binding, and activator.

A total of 134 KEGG signaling pathways were identified. The top 15 enriched pathways were chosen, and histograms were plotted considering P values, Q values, and gene counts, as illustrated in Figure 5B. Notably, the phosphatidylinositol 3-kinase/serine-threonine kinase (PI3K-Akt) signaling pathway, the mitogen-activated protein kinase (MAPK) signaling pathway, regulation of the actin cytoskeleton, and focal adhesion were the predominant pathways involved in the treatment of MAC with DJD.

https://doi.org/10.1021/acsomega.4c03641
ACS Omega 2024, 9, 28926−28936

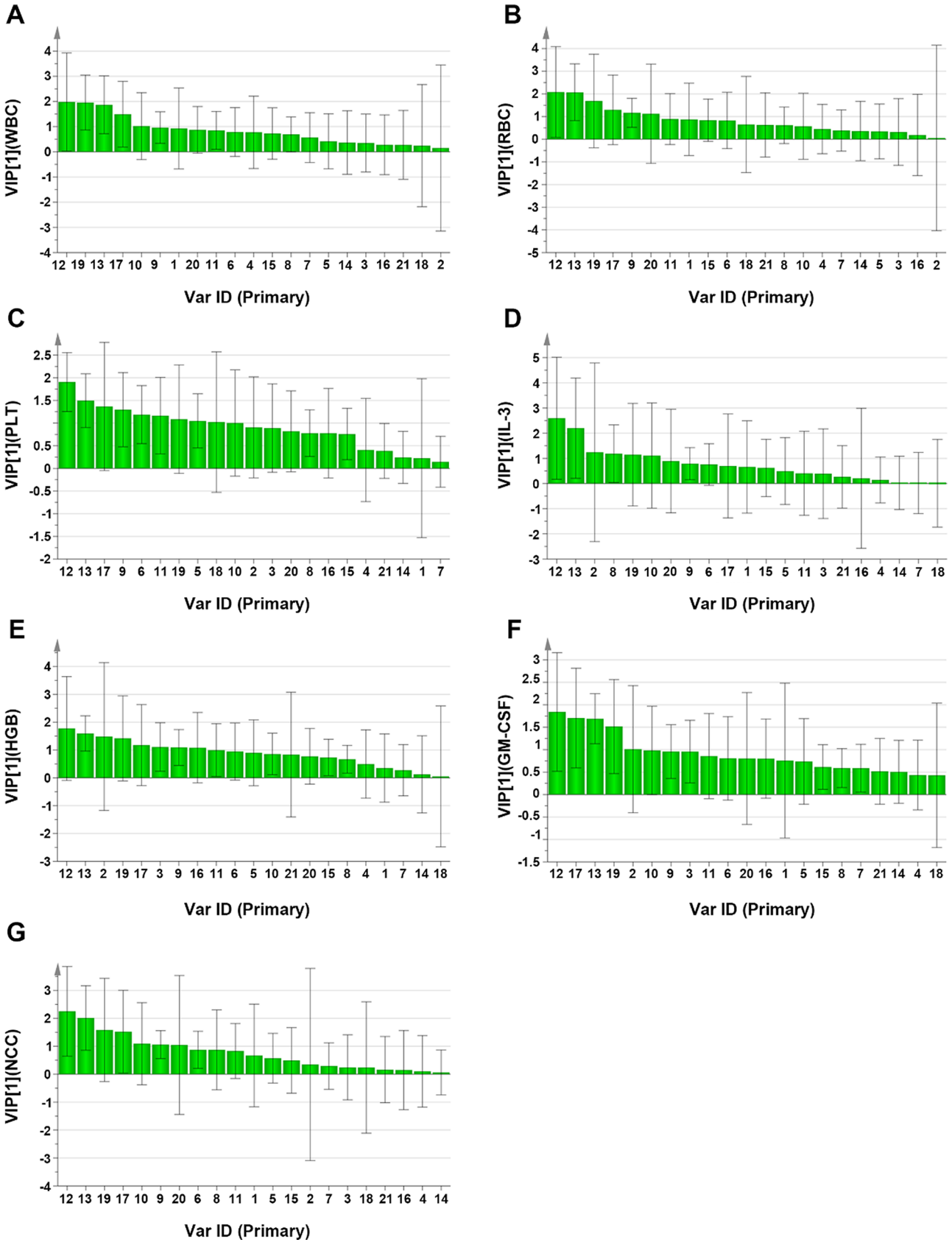

Figure 3. OPLS-DA results of common peaks and each pharmacodynamic index of DJD. VIP values between the common peaks and peripheral blood markers in rats with MAC. (A) WBC, (B) RBC, (C) PLT, (D) IL-3, (E) HGB, (F) GM-CSF, and (G) NCC (mean ± SD, $n = 6$).

qPCR Testing. To confirm the above results, qPCR was utilized to determine the expression levels of the PTK2, AKT, and PI3K genes in rat bone marrow cells. Figure 6 shows that the expression levels of PTK2, AKT, and PI3K mRNA in the model

https://doi.org/10.1021/acsomega.4c03641
ACS Omega 2024, 9, 28926−28936

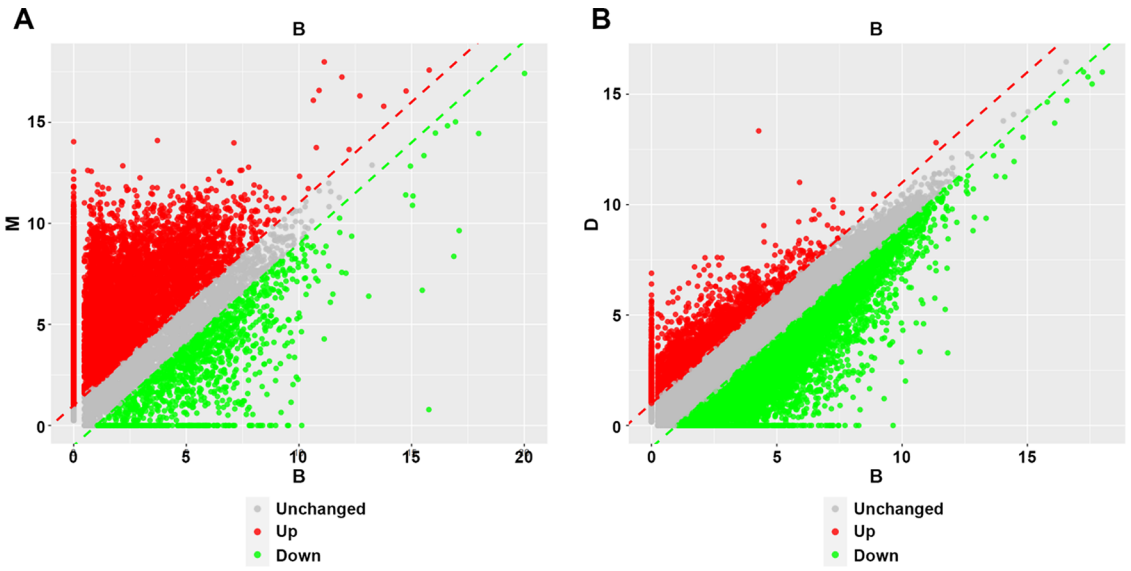

Figure 4. Volcano of differential gene expression in each group. (A) Control group vs model group. (B) Model group vs DJD group.

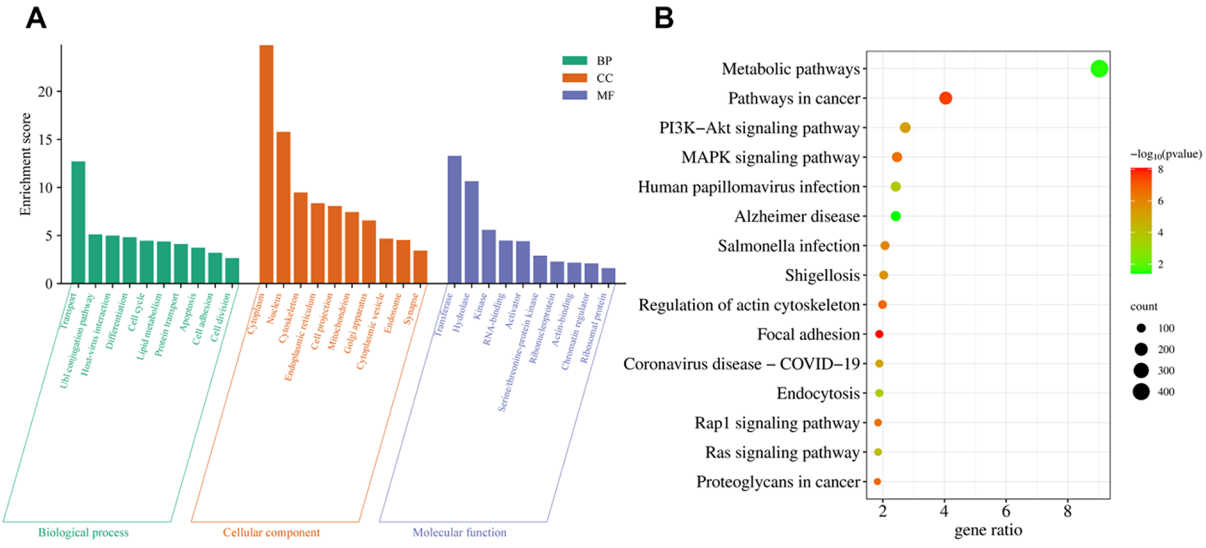

Figure 5. Screening and enrichment analysis of differentially expressed genes. (A) GO enrichment analysis plot of differentially expressed genes. (B) KEGG enrichment analysis plot of differentially expressed genes.

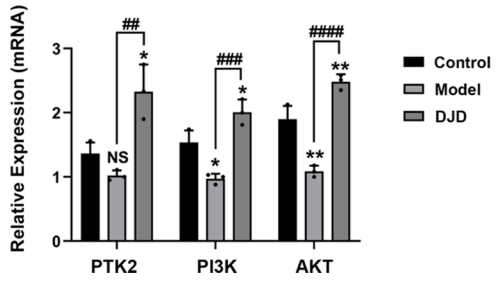

Figure 6. Expression of the PTK2, PI3K, and AKT genes in the bone marrow cells of the rats (mean ± SD, $n = 3$). NS: $p > 0.05$, $^{*}p < 0.05$, $^{**}p < 0.01$, compared with the control group; $^{\#\#}p < 0.01$, $^{\#\#\#}p < 0.001$, $^{\#\#\#\#}p < 0.0001$, compared with the model group; ANOVA.

group were significantly lower than those in the control group ($P < 0.01$, $P < 0.05$). However, the expression of PTK2, AKT, and PI3K mRNA in the DJD group was significantly increased ($P < 0.01$), which was consistent with the results of the RNA-Seq analysis. This finding suggested that the mechanism by which DJD treats MACs is related to the disruption of cell adhesion and the regulation of the PI3K-Akt signaling pathway.

DISCUSSION

As a common adverse reaction during chemotherapy, MAC mainly manifests as anemia, increased risk of bleeding, and infections, which seriously affect the quality of life and prognosis of patients and may ultimately influence long-term clinical efficacy and reduce disease-free survival and overall survival.[19,20] Some Chinese medicines (e.g., ginseng, Astragalus, and *Panax ginseng*) are often used in combination with chemotherapy or radiotherapy, which can improve therapeutic efficacy and alleviate the side effects and complications caused by chemotherapy and radiotherapy while reducing the cost of treatment.[4,21] Huan et al. demonstrated that a Chinese herbal decoction, Jian Wei Xiao Shi decoction combined with Yi Qi Bu Xue decoction, could reduce the incidence of chemotherapy-induced leukopenia, neutropenia, and febrile neutropenia in

https://doi.org/10.1021/acsomega.4c03641
ACS Omega 2024, 9, 28926−28936

breast cancer patients.[22] Zhao et al. proved in a randomized controlled trial that Six-flavored Dihuang decoction and Yi Qi Bu Xue decoction exhibited obvious protective effects on peripheral blood leukopenia caused by chemotherapy or radiotherapy and significantly increased the number of hematopoietic stem cells.[9] In a preliminary study, we verified the therapeutic effect of DJD on MAC by constructing a rat model and exploring the core targets, key compounds, major biological processes, and signaling pathways related to treatment. However, due to the large number of components and the complexity of the ingredients, it is difficult to confirm the active ingredients and evaluate the dose−effect relationships of Chinese herbal tonics.

In this study, the fingerprints of DJD were established by UPLC-MS. Each batch of DJD contained 21 common peaks, and the similarity between the fingerprints was greater than 0.92. On the basis of the common peaks, we carried out a gray correlation analysis by integrating the seven indicators of efficacy and found that there were eight peaks with greater correlations with efficacy, namely, peaks 2, 7, 10, 14, 15, 16, 18, 21, 18, and 21. Considering the positive correlation between the dose and efficacy of DJD in previous studies, we performed partial least-squares regression analysis around the 21 common peaks and discovered that there were four shared peaks with VIP values greater than 1, namely, 10, 12, 13, and 19. Overall, we tentatively confirmed that the main active ingredients exerting therapeutic efficacy in DJD were albiflorin (10), paeoniflorin (12), galloylpaeoniflorin (13), salvianolic acid H/I (14), albiflorin R1 (16), salvianolic acid B (18), salvianolic acid E (19), benzoylpaeoniflorin (21), and $C_{12}H_{18}N_5O_4$ (2).

As an important component of DJD, Baishao, which contains paeoniflorin and benzoylpaeoniflorin, has been proven by several studies to be therapeutic for both bone marrow suppression and iron deficiency anemia induced by radiotherapy and chemotherapy.[23] In addition, benzoylpaeoniflorin has antiallergic potential by inhibiting the HDC and MAPK signaling pathways[24] and can attenuate septicemia in model rats by activating anti-inflammatory mechanisms.[25] Through selective inhibition of organic cation transporter 1, benzoylpaeoniflorin can alleviate hepatic lipid accumulation by activating AMPK.[26] In addition to its therapeutic effects on postchemotherapy myelosuppression,[27] paeoniflorin can improve memory deficits in APP/PS1 transgenic mice by improving mitochondrial dysfunction[28] and has antidepressant potential.[29] Yao Yan et al. reported that salvianolic acid can inhibit ADP-induced platelet aggregation,[30] and Ho et al. summarized the multiple mechanisms of cardiovascular protection by salvianolic acid.[31]

There are several limitations to this study. First, the components we detected were mainly from *Paeonia lactiflora*, *Salvia miltiorrhiza*, and *Spatholobi caulis* but fewer were from *Radix Rehmanniae* Praeparata, *Radix Angelicae* Sinensis, and *Longan Fructus*. For peak 2, which was derived from longan and is closely related to the therapeutic effect, we could only identify its chemical formula as $C_{12}H_{18}N_5O_4$, and its specific composition still needs to be further investigated. Second, due to the influence of detection conditions and sample extraction, the components identified in different studies may be slightly different. Nevertheless, terpenoids in *Paeonia lactiflora*, phenolic acids in *Salvia miltiorrhiza* , and polyphenols in *Spatholobi caulis* play important roles in the treatment of MAC. In future studies, more attention should be given to the pharmacodynamic components of TCM, which are in line with the multitarget and multicomponent therapeutic characteristics of TCM.

RNA-Seq allows researchers to fully observe and analyze the level of gene expression in cells or tissues.[32] It also enables researchers to determine how drugs affect gene expression, including whether a given drug can activate or inhibit the expression of a particular gene.[33] Finally, RNA-Seq can reveal how drugs affect signal transduction pathways.[34] With a length of approximately 200 nucleotides, lncRNAs are noncoding RNAs that exhibit strong tissue and species selectivity.[35] Through splicing mRNA, gene transcription regulation, post-transcriptional translation, and modification, it can control the expression of target genes.[36]

In this work, RNA-Seq was utilized to identify differentially expressed genes, and KEGG enrichment analysis was performed. The mechanism by which DJD prevents and treats MAC was linked to the PI3K-Akt signaling pathway, MAPK signaling pathway, regulation of the actin cytoskeleton, and focal adhesion. Focal adhesion is a structure composed of integrin protein (ITG), which contributes to cell structure stability, regulates cell signal transmission, promotes cell contact, and participates in biological processes such as cell migration, proliferation, and differentiation.[37] The focal adhesion structure of cells contains focal adhesion kinase (PTK2), and its interaction with ITG can initiate a series of signal transduction cascade processes, hence influencing cell function and behavior.[38] To summarize, modulating ITG/PTK2 activity and behavior in cell matrix adhesion and signal transduction is critical for optimizing cell−microenvironment interactions and preventing and treating bone marrow suppression following chemotherapy. As a result, DJD can restore damaged cell function and enhance the hematopoietic microenvironmental balance by interfering with the PI3K-Akt signaling pathway, enhancing the recovery of bone marrow hematological function.

CONCLUSIONS

Overall, this study established the fingerprints of DJD by UPLC-MS. Based on the common peaks screened by the fingerprint profile, this study preliminarily identified the main active ingredients exerting therapeutic effects on DJD by using gray correlation and partial least-squares regression analyses. The prevention and treatment of MAC by DJD are linked to the modulation of the PI3K-Akt signaling pathway and the improvement of hematopoietic microenvironmental homeostasis.

ASSOCIATED CONTENT

Supporting Information

The Supporting Information is available free of charge at https://pubs.acs.org/doi/10.1021/acsomega.4c03641.

The results of DJD in the treatment of MAC (Table S1) and the results of gray relational analysis (Tables S2−S8) (PDF)

AUTHOR INFORMATION

Corresponding Authors

Zhanyun Ren − *The Affiliated Yixing Hospital of Jiangsu University, Yixing 214200, China*; Email: staff1003@yxph.com

Zhiqiang Hu − *The Affiliated Yixing Hospital of Jiangsu University, Yixing 214200, China*; orcid.org/0009-0008-8662-2623; Email: Hzqscig@163.com

https://doi.org/10.1021/acsomega.4c03641
ACS Omega 2024, 9, 28926−28936

Authors

Mingxin Guo − *The Affiliated Yixing Hospital of Jiangsu University, Yixing 214200, China*

Jiaqi Zeng − *The Affiliated Yixing Hospital of Jiangsu University, Yixing 214200, China*

Jing Li − *Zibo Central Hospital, Zibo 255000, China*

Luyao Jiang − *The Affiliated Yixing Hospital of Jiangsu University, Yixing 214200, China*

Xia Wu − *Guangdong Pharmaceutical University, Guangzhou 516006, China*

Complete contact information is available at: https://pubs.acs.org/10.1021/acsomega.4c03641

Author Contributions

Z.H.: conceptualization. Z.R.: formal analysis. M.G. and J.Z.: writing-original draft and visualization. W.F.: conceptualization. L.J.: resources. X.W.: writing-review and editing. T.M.: supervision. All of the authors reviewed and approved the final manuscript. M.G. and J.Z. contributed equally to this work.

Funding

The authors acknowledge the support received from the Foundation of Wuxi Administration of Traditional Chinese Medicine (grant number: ZYYB29).

Notes

The authors declare no competing financial interest.

■ ABBREVIATIONS

MAC	myelosuppression after chemotherapy
DJD	Danggui Jixueteng Decoction
RNA-seq	transcriptome sequencing technologies
UPLC-MS	ultraperformance liquid chromatography-mass spectrometry
WBC	white blood cell count
RBC	red blood cell count
PLT	platelet count
IL-3	interleukin-3
HGB	hemoglobin concentration
GM-CSF	granulocyte-macrophage colony-stimulating factor
NCC	nucleated cell count
GO	Gene Ontology
KEGG	Kyoto Encyclopedia of Genes and Genomes
UPLC/Q-TOF-MS	ultraperformance liquid chromatography coupled with Q-TOF mass spectrometry
RSD	relative standard deviation
GRA	gray relational grade analysis
PLSR	partial least-squares regression
PPI	construction of protein−protein interaction network
VIP	variable importance in projection
BP	biological process
CC	cell component
MF	molecular function
ITG	integrin protein
PTK2	focal adhesion kinase

■ REFERENCES

(1) Xia, C.; Dong, X.; Li, H.; Cao, M.; Sun, D.; He, S.; Yang, F.; Yan, X.; Zhang, S.; Li, N.; Chen, W. Cancer statistics in China and United States, 2022: profiles, trends, and determinants. *Chinese Med. J.* **2022**, *135* (05), 584−590.

(2) Pearce, A.; Haas, M.; Viney, R.; Pearson, S.-A.; Haywood, P.; Brown, C.; Ward, R. Incidence and severity of self-reported chemotherapy side effects in routine care: A prospective cohort study. *PloS one* **2017**, *12* (10), No. e0184360.

(3) Wang, X.; Zhang, X.; Zhang, Y.; Xia, L. The effect of acupuncture and selection of acupoints on myelosuppression after chemotherapy. *TMR Non-Drug Ther* **2022**, *5* (2), 9.

(4) He, M.; Wang, N.; Zheng, W.; Cai, X.; Qi, D.; Zhang, Y.; Han, C. Ameliorative effects of ginsenosides on myelosuppression induced by chemotherapy or radiotherapy. *Journal of Ethnopharmacology* **2021**, *268*, No. 113581.

(5) Ji, Y.; Li, S.; Zhang, X.; Liu, Y.; Lu, Q.; Li, Q.; Chen, W.; Sheng, J.; Jiang, K.; Liang, H.; Sha, S.; Li, M.; Chen, Z.; Zheng, P.; Wang, M.; Feng, Y.; Wang, L.; Wu, H.; Liu, H.; Huang, Y.; Yin, Z.; Xue, X. The prophylactic and therapeutic effects of moxibustion combined with traditional Chinese medicine decoction for treating chemotherapy-induced myelosuppression in early-stage breast cancer: study protocol for a randomized controlled trial. *Trials* **2020**, *21*, 844.

(6) Zhao, Z.; Zhang, X.; Zeng, Q.; Su, H. Treatment of periarthritis of shoulder joint by moxibustion combined with Danggui Jixueteng decoction in 30 cases. *Guiding J. Tradit. Chinese Med. Pharmacol.* **2011**, *17* (8), 64−65.

(7) Cho, J.; Cho, C.; Shin, J.; Son, J.; Kang, W.; Son, C. Myelophil, an extract mix of Astragali Radix and Salviae Radix, ameliorates chronic fatigue: a randomised, double-blind, controlled pilot study. *Complementary Therapies in Medicine* **2009**, *17* (3), 141−146.

(8) Peng, F.; Hong, W.; Wang, Y.; Peng, Y.; Fang, Z. Mechanism of herb pair containing Astragali Radix and Spatholobi Caulis in the treatment of myelosuppression based on network pharmacology and experimental investigation. *Journal of Ethnopharmacology* **2024**, *319*, No. 117178.

(9) Jia, Y.; Du, H.; Yao, M.; Cui, X.; Shi, Q.; Wang, Y.; Yang, Y. Chinese herbal medicine for myelosuppression induced by chemotherapy or radiotherapy: a systematic review of randomized controlled trials. *Evidence-Based Complem. Altern. Med.* **2015**, *2015*, No. 690976, DOI: 10.1155/2015/690976.

(10) Xiao, H.; Xiong, L.; Song, X.; Jin, P.; Chen, L.; Chen, X.; Yao, H.; Wang, Y.; Wang, L. Angelica sinensis polysaccharides ameliorate stress-induced premature senescence of hematopoietic cell via protecting bone marrow stromal cells from oxidative injuries caused by 5-fluorouracil. *International journal of molecular sciences* **2017**, *18* (11), 2265.

(11) Guo, M.; Zeng, J.; Li, W.; Hu, Z.; Shen, Y. Danggui Jixueteng decoction for the treatment of myelosuppression after chemotherapy: A combined metabolomics and network pharmacology analysis. *Heliyon* **2024**, *10* (3), No. e24695, DOI: 10.1016/j.heliyon.2024.e24695.

(12) Li, C.-J.; Zhai, R.-R.; Zhu, X.-Y.; Guo, Z.-F.; Yang, H. Discovery of effective combination from Renshen-Fuzi herbal pair against heart failure by spectrum-effect relationship analysis and zebrafish models. *Journal of Ethnopharmacology* **2023**, *317*, No. 116832.

(13) Liu, X.; Wang, Y.; Ge, W.; Cai, G.; Guo, Y.; Gong, J. Spectrum−effect relationship between ultra-high-performance liquid chromatography fingerprints and antioxidant activities of Lophatherum gracile Brongn. *Food Science & Nutrition* **2022**, *10* (5), 1592−1601.

(14) Zhe, C. S.; Lin, Z. J.; Xiao, M. L.; Niu, H. J.; Zhang, B. The spectrum-effect relationship-a rational approach to screening effective compounds, reflecting the internal quality of Chinese herbal medicine. *Chinese J. Nat. Med.* **2016**, *14* (3), 177−184.

(15) Xu, G.-L.; Xie, M.; Yang, X.-Y.; Song, Y.; Yan, C.; Yang, Y.; Zhang, X.; Liu, Z.-Z.; Tian, Y.-X.; Wang, Y.; Jiang, R.; Liu, W.-R.; Wang, X.-H.; Shi, G.-M. Spectrum-effect relationships as a systematic approach to traditional Chinese medicine research: current status and future perspectives. *Molecules* **2014**, *19* (11), 17897−17925.

(16) Zhu, G. L.; Wang, B.; Feng, G.; Huang, A.-X.; Yin, G.; Wang, S. H.; Su, H. M.; Wang, W. J.; Wang, P.; Yu, X. A. Exploring the processing-related components from asparagi radix via diversified spectrum-effect relationship. *Chinese J. Anal. Chem.* **2023**, *51* (2), No. 100214.

(17) Song, Y.; Yang, J.; Hu, X.; Gao, H.; Wang, P.; Wang, X.; Liu, Y.; Cheng, X.; Wei, F.; Ma, S. A stepwise strategy integrating metabolomics and pseudotargeted spectrum−effect relationship to elucidate the potential hepatotoxic components in Polygonum multiflorum. *Frontiers in pharmacology* **2022**, *13*, No. 935336.
(18) Tang, L.; Zhao, H.-Q.; Yang, H.; Hu, C.; Ma, S.-J.; Xiao, W.-Z.; Qing, Y.-H.; Yang, L.; Zhou, R.-R.; Liu, J.; Zhang, S.-H. Spectrum−effect relationship combined with bioactivity evaluation to discover the main anxiolytic active components of Baihe Dihuang decoction. *J. Ethnopharmacol.* **2024**, *319*, No. 117090.
(19) Pettengell, R.; Johnson, H. E.; Lugtenburg, P. J.; Silvestre, A. S.; Dührsen, U.; Rossi, F. G.; Schwenkglenks, M.; Bendall, K.; Szabo, Z.; Jaeger, U. Impact of febrile neutropenia on R-CHOP chemotherapy delivery and hospitalizations among patients with diffuse large B-cell lymphoma. *Supportive Care in Cancer* **2012**, *20*, 647−652.
(20) Yang, S.; Che, H.; Xiao, L.; Zhao, B.; Liu, S. Traditional Chinese medicine on treating myelosuppression after chemotherapy: A protocol for systematic review and meta-analysis. *Medicine* **2021**, *100* (4), No. e24307.
(21) Park, B.; Noh, H.; Choi, D.-J. Herbal medicine for xerostomia in cancer patients: a systematic review of randomized controlled trials. *Integrative cancer therapies* **2018**, *17* (2), 179−191.
(22) Tian, H.; Qin, W.; Wu, W.; Guo, P.; Lu, Y.; Liu, P.; Liu, Q.; Su, F. Effects of traditional Chinese medicine on chemotherapy-induced myelosuppression and febrile neutropenia in breast cancer patients. *Evidence-Based Complem. Altern. Med.* **2015**, *2015*, No. 736197, DOI: 10.1155/2015/736197.
(23) Ye, X.-W.; Deng, Y.-L.; Xia, L.-T.; Ren, H.-M.; Zhang, J.-L. Uncovering the mechanism of the effects of Paeoniae Radix Alba on iron-deficiency anaemia through a network pharmacology-based strategy. *BMC Complem. Med. Ther.* **2020**, *20* (1), 130.
(24) Zhong, W.-C.; Li, E. C.; Hao, R. R.; Zhang, J.-F.; Jin, H.-T.; Lin, S. Anti-anaphylactic potential of benzoylpaeoniflorin through inhibiting HDC and MAPKs from Paeonia lactiflora. *Chinese J. Nat. Med.* **2021**, *19* (11), 825−835.
(25) Kim, C.; Sim, H.; Bae, J.-S. Benzoylpaeoniflorin activates anti-inflammatory mechanisms to mitigate sepsis in cell-culture and mouse sepsis models. *International Journal of Molecular Sciences* **2022**, *23* (21), 13130.
(26) Bi, Y.; Wang, X.; Han, L.; Tian, Y.; Bo, T.; Li, C.; Shi, B.; Gui, C.; Zhang, Y. Selective Inhibition of Organic Cation Transporter 1 by Benzoylpaeoniflorin Attenuates Hepatic Lipid Accumulation through AMPK Activation. *J. Nat. Prod.* **2023**, *86* (1), 191−198.
(27) Zhu, Y.-L.; Wang, L.-Y.; Wang, J.-X.; Wang, C.; Wang, C. L.; Zhao, D. P.; Wang, Z.-C.; Zhang, J.-J. Protective effects of paeoniflorin and albiflorin on chemotherapy-induced myelosuppression in mice. *Chinese J. Nat. Med.* **2016**, *14* (8), 599−606.
(28) Xu, Y.-J.; Mei, Y.; Shi, X.-Q.; Zhang, Y.-F.; Wang, X.-Y.; Guan, L.; Wang, Q.; Pan, H.-F. Albiflorin ameliorates memory deficits in APP/PS1 transgenic mice via ameliorating mitochondrial dysfunction. *Brain research* **2019**, *1719*, 113−123.
(29) Zhao, Z.-X.; Fu, J.; Ma, S.-R.; Peng, R.; Yu, J.-B.; Cong, L.; Pan, L.-B.; Zhang, Z.-G.; Tian, H.; Che, C.-T. Gut-brain axis metabolic pathway regulates antidepressant efficacy of albiflorin. *Theranostics* **2018**, *8* (21), 5945−5959.
(30) Yao, Y.; Wu, W.-Y.; Liu, A.-H.; Deng, S.-S.; Bi, K.-S.; Liu, X.; Guo, D.-A. Interaction of salvianolic acids and notoginsengnosides in inhibition of ADP-induced platelet aggregation. *American journal of Chinese medicine* **2008**, *36* (02), 313−328.
(31) Ho, J. H.-C.; Hong, C.-Y. Salvianolic acids: small compounds with multiple mechanisms for cardiovascular protection. *J. Biomed. Sci.* **2011**, *18*, 30.
(32) Zhang, J.; Peng, G.; Chi, H.; Yang, J.; Xie, X.; Song, G.; Tran, L. J.; Xia, Z.; Tian, G. CD8-T-cell marker genes reveal different immune subtypes of oral lichen planus by integrating single-cell RNA-seq and bulk RNA-sequencing. *BMC Oral Health* **2023**, *23* (1), 464.
(33) Cai, S.; Hu, B.; Wang, X.; Liu, T.; Lin, Z.; Tong, X.; Xu, R.; Chen, M.; Duo, T.; Zhu, Q.; Liang, Z.; Li, E.; Chen, Y.; Li, J.; Liu, X.; Mo, D. Integrative single-cell RNA-seq and ATAC-seq analysis of myogenic differentiation in pig. *BMC Biol.* **2023**, *21* (1), 19.
(34) Zheng, K.; Lin, L.; Jiang, W.; Chen, L.; Zhang, X.; Zhang, Q.; Ren, Y.; Hao, J. Single-cell RNA-seq reveals the transcriptional landscape in ischemic stroke. *Journal of Cerebral Blood Flow & Metabolism* **2022**, *42* (1), 56−73.
(35) Jiang, N.; Zhang, X.; Gu, X.; Li, X.; Shang, L. Progress in understanding the role of lncRNA in programmed cell death. *Cell Death Discovery* **2021**, *7* (1), 30.
(36) Zhao, T.; Hu, Y.; Peng, J.; Cheng, L. DeepLGP: a novel deep learning method for prioritizing lncRNA target genes. *Bioinformatics* **2020**, *36* (16), 4466−4472.
(37) Kadry, Y. A.; Calderwood, D. A. Structural and signaling functions of integrins. *Biochimica et Biophysica Acta (BBA)-Biomembranes* **2020**, *1862* (5), No. 183206.
(38) Mishra, Y. G.; Manavathi, B. Focal adhesion dynamics in cellular function and disease. *Cellular signalling* **2021**, *85*, No. 110046.

https://doi.org/10.1021/acsomega.4c03641
ACS Omega 2024, 9, 28926−28936